Volume 9, Issue 2, 2020, 945 - 951 **ISSN 2284-6808**

Letters in Applied NanoBioScience

https://nanobioletters.com/

https://doi.org/10.33263/LIANBS92.945951

Original Review Article **Open Access Journal**

Received: 17.01.2020 / Revised: 27.03.2020 / Accepted: 27.03.2020 / Published on-line: 30.03.2020

A review on formulation, design of nanostructured material through oil-in-water micro-emulsion

Rasmita Nayak [1], Binita Nanda [1,*]

[1]Department of Chemistry, Institute of Technical Education and Research, Siksha 'O' Anusandhan (Deemed to be University), Bhubaneswar, Odisha, India

*corresponding author e-mail address: ***binitananda@soa.ac.in*** | Scopus ID 53980125400

ABSTRACT

The nanostructured materials are the basic scientific interest in the research community. The properties of nanostructured materials with their variable sizes, shapes and reduced dimensions boost their performance towards wide variety of applications concomitant to electronics, optoelectronics, sensors, photocatalysis, and biomedical field. Among all the established methods to design nano structured materials, micro-emulsion has attained a significant role because of its unique properties like thermodynamically stability, ultralow interfacial tension, and large interfacial area. Apart from its versatility, microemulsion is one of the most cost effective and environmentally benign preparation method which can control the particle size, geometry, morphology, homogeneity, and surface area of nano structured materials. This review article focuses on the recent development in the above area, various factors that influence the oil-in water micro-emulsion (µ-emulsion) to formulate different shapes and size of nano structured materials.

Keywords: *µ-emulsion; o@w, nucleation; self-assembly process; crystal-growth; nanoparticle formation.*

1. INTRODUCTION

For the first time on December 29, 1959 the idea of nanotechnology appeared in the famous talk of the physicist Richard Feynman at the American Physical Society meeting at Caltech "*there is plenty of room at the bottom"* [1]. Shape controlled nanostructured materials are the hot topic among the researchers, scientists because of its versatile utility towards catalysis, drug delivery, photography, photonics, electronics, labeling, imaging, sensing and surface enhanced Raman scattering [2,3]. According to Royal Society UK, nanostructured materials are the manipulation of materials at atomic, molecular, and macromolecular level, but shows significantly large scale properties. The synthesis procedure, design and characterization decide the structure of nanomaterial. Generally, nanostructured materials deal with sizes between 1-100 nm in dimension. The properties of nanostructures material are different from the bulk material because of the large active sites and high surface to volume ratio and a possible appearance of quantum effect at the nanoscale. Because of the scientific and industrial importance the size and shape effects of nanostructured materials have attracted enormous attention to the common society [4].

The size and shape of a material can influence the physicochemical properties [5]. Various physical properties of a material such as color, melting point, magnetic and electronic properties, catalysis, chemical bond formation and surface hydrophilicity/hydrophobicity etc. are size dependent. Size control allows modification of these properties in a large range and leads to development in materials science, comparable to a third dimension in a periodic table. So far, a number of works have done by the scientists on size dependent nanoparticles [6-8]. Chen et al. showed characteristic absorption colors and properties of Au NP with variation in shape and size and utilization in bio-imaging, drug delivery, biosensing and photothermal therapy applications. The percentage of gold concentration and nanoshell thickness responsible for changing the color of the Au NP solution [9]. M. V. Fuke and his team studied the variation in particle size of silver nanoparticles for better application in sensor. Smaller the particle size of Ag nanoparticle opens more sites for interaction of water molecules give more sensitivity and also for higher particle size the number of voids reduces offering low sensitivity [10]. Gross et al. detected the particle size and concentration of different sized NPs in suspensions of polymer and protein samples [11]. Nanostructured materials synthesis and maintaining their physical properties like mechanical rigidity, thermal stability or chemical inactivity is a challenge to the scientific community. Different physical and chemical methods like hydrothermal, sol gel, impregation, precipitation, solid state dispersion, reflux, co-assembly, chemical reduction, thermal irradiation, and micro-emulsion have been employed for the synthesis of different dimensional inorganic and organic nanostructured materials [12-16]. Amongst these, µ-emulsion is one of the best method to synthesize nanostructured materials of different size and shape because of its cost effectiveness, environmentally friendly adaptable preparation method which control the size, geometry, morphology, homogeneity and surface area of the nanoparticles [17-19].

In 1959, µ-emulsion method was first coined by J. H. Schulman and since then its use has been developed considerably and has received justified acclamation from the nanomaterial community [20]. Among all the synthetic approach to give a proper shape and size of the nanomaterials, µ-emulsion is an ideal technique for the preparation of inorganic nanoparticles of size range between 10-100 nm. It is thermodynamically stable, macroscopically homogeneous, isotropic dispersion and optically transparent as compared to emulsion. µ-emulsion has taken a special interest because different precursors (reactants) can be inserted into the nanosized aqueous domains leading to materials

of different shape and size. That means the size and shape of the droplets select the size and shape of nanomaterials [21-23]. Depending on the hydrophilic–lypophilic balance (HLB) value of the used surfactant proportion, μ-emulsions can be classified as oil-in-water (o@w), w@o or reverse μ-emulsion, and intermediate bicontinuous structural types [24, 25].

Among three μ-emulsion types, an o@w μ-emulsion (comprised of oil, surfactant and co-surfactant) is a thermodynamically stable colloidal dispersion system is shown in scheme 1. In o@w μ-emulsion oil is dispersed phase and water is continuous phase and the percentage of oil is low as compared to water. During the physicochemical mechanism the movement of a water-miscible component (either solvent or surfactant) from the organic phase into the aqueous phase occurs and a large turbulent force at the interface of o@w occur. This causes a large increase in the oil–water interfacial area, which leads to the spontaneous formation of oil droplets surrounded by aqueous phase through a budding process. That means the surfactant molecules are organized so that their nonpolar tails associated with each other forming a hydrophobic core because the charged head group droplet is the driving force for producing o@w μ-emulsion. At first, surfactant molecule miscible in water medium to form micelles which depend on the structure of surfactants that is balance in size between hydrophobic head and hydrophilic tail. In aqueous phase the micelles containing polar head groups usually from the outside of the micelles. This proves that polar head group (hydrophobic head) faces towards the water phase and the nonpolar (hydrophilic tail) is towards the oil phase.

Different nanostructure like spheroid, cylinder or rod like structure can be designed by changing one of these parameters (the water content, water to surfactant ratio, amount of oil, types of surfactants and co-surfactants) within these phase.

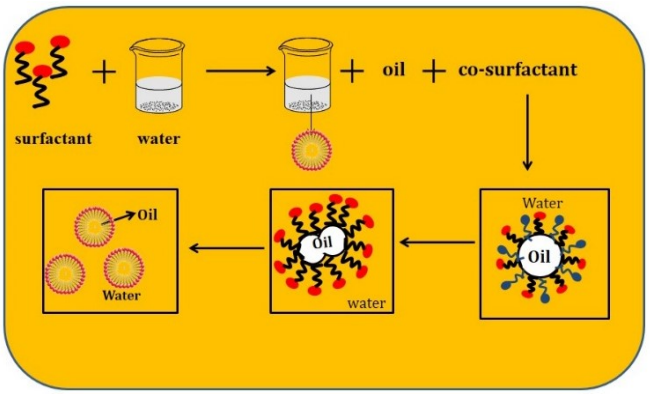

Scheme-1. Schematic representation of o@w μ-emulsion.

To date a number of established μ-emulsion methods have been used by scientists, researchers for the fabrication of materials [26]. Hao and his co-workers synthesized zinc nickel ferrite nanorod (50-200 nm in diameter) through o@w μ-emulsion method using CTAB as surfactant, n-pentanol as co-surfactant and extensively studied about their magnetic properties [27,28].

In this present manuscript we primarily concern for the shape and size variation through o@w μ-emulsion method. The synthesis, nucleation and growth of the grain size are the major steps to attain a specific shape and variable sizes of nanomaterials. Keeping all these in our mind the review summarizes some recent works on micro-emulsion methods to determine the exact shape with variable sizes by changing water to surfactant ratio, varying oils and co-surfactants, pH and temperature.

2. ROLE OF MICRO-EMULSION IN NANOMATERIAL FABRICATION

In the future development, the synthetic control of size of nanoparticles, comprising the porosity, diameter, encapsulations are valuable. Compared to other synthetic methods, μ-emulsion is a thermodynamically equilibrium system and the size of the droplets is typically uniform [29]. In principle, the size can be controlled systematically by changing inter facial curvature through surfactant/co-surfactant composition or solution condition [30, 31]. Oil, surfactant and water in the μ-emulsion process help in the formation of micelles. Continuous collide, coalesce form micelles and at the same time exchange of the solution occur. Variation of sizes and shape of the nanostructured materials during synthesis mainly depend on nucleation, growth and solubility as per La mer et al. as shown in scheme 2 [32]. At first in the reaction medium during precipitation, the concentration increases with time and when it reaches the super saturation value starts nucleation. After nucleation, there is a gradual decrease in the concentration. This decrease in concentration is due to the growth of the particle and it retains until the concentration reaches the solubility value. Then the entire process is well suitable in emulsion medium and the size of the particle will increase continuously with an increase in the concentration of the precursor. This is clearly explained in the scheme 2. Again the use of surfactants in the μ-emulsion system stabilizes the nanoparticle thermodynamically [32]. The size of the nanoparticles depends upon the inter micellar exchange, which is affected by the various factors such as the types of solvent, the type of surfactant, type of co-surfactants and the water to surfactant ratio.

2.1. Type of oil/solvent.

The oil or solvents play significant role in the assemblage of the surfactant molecules. It is because, in nanoparticle formation, there is an interaction between the solvent and surfactant tail. The growth rate of nanoparticle is hampered due to the bulkiness of solvent molecule. The bulkiness of the solvent molecules are in the order of n propane < n-butane < n-pentane < n-hexane < cyclohexane <iso-octane. As the chain length of the solvent molecule (n) increases, growth rate gradually decreases and hence size of the nanoparticle increases. This is attributed to the variation in the intermicellar exchange rate which is given by the degree of interaction of solvent molecule with the surfactant tails. Precisely, in o@w μ-emulsion, oil molecule having lesser molecular volume, can enter between the tails of the surfactant molecule and increases the rigidity and curvature of the surfactant. Again the growth rate is hindered with an increase in rigidity and the size of the nanoparticle increases. This is due to the presence of free water in the micellar pool and from this, it is clear that water level (Wo) has a key role in the growth rate and determining the size. So, with an increase in chain length of the solvent molecule at constant water level (Wo) the size of the nanoparticle gradually increases. But in case of short chain alkanes, they are easily penetrate deeper into the micellar shell and spread and became apart from the surfactant molecule. As a result there is a decrease

in free water concentration inside the micelle decreases which again decreases the size of the nanoparticles. Thus the penetrability of oil into the micellar shells decides the growth is largely controlled at initial stage while the amount of water in micellar pool decides the size.

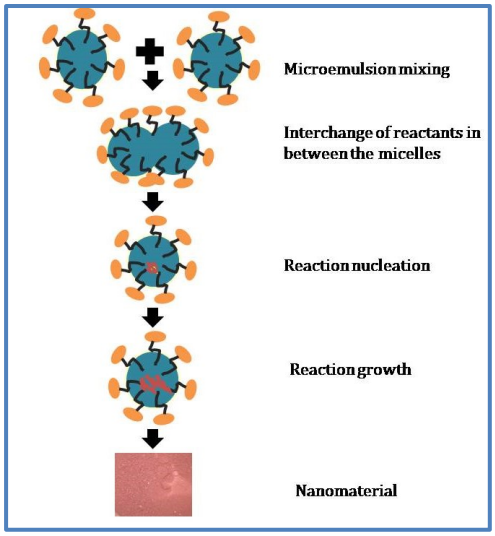

Scheme 2. Schematically representation of sequential steps involved in synthesis process of nanomaterial.

2.2. Type of surfactant.

Surfactants or ampiphiles have an important role in micro-emulsion process. It stabilizes the oil/water phase (immiscible) by reducing the interfacial tension. Different parameters of surfactant that decide the type, shape and structure are: i) hydrophilic lipophilic balance (HLB) value, ii) critical micelle concentration (CMC) and iii) surfactant packing parameter (Ns). At first the surfactants having hydrophilic head and hydrophobic tail that forms aggregation in solvent and held by van-der waals' interaction [33]. They are cationic (CTAB), anionic (SDS, AOT), zwitter ionic or nonionic (Triton X-100, CA-520, NP-5, Igepal) depending on the nature of head group (HLB balance). The HLB number of surfactants also decides the type of micro-emulsion one can get. The most lipophilic molecule was assigned to HLB number 1, while most hydrophobic molecules have HLB number 20. For example o@w µ-emulsion obtained at higher HLB value whereas w@o µ-emulsion depends upon the low HLB number. Secondly, when the concentration of surfactants is greater than CMC, a micelle formed. During micellization, there is a transfer of non-polar surfactant chains from an ordered aqueous environment to the hydrocarbon like environment of the micelle, resulting disordering the water molecular surrounding the non-polar molecules. Thereby increasing the entropy of the system and stabilizing the µemulsion. At last, surfactant packing parameter (Ns), mainly depend upon the volume of hydrocarbon head group and length of chain are given by the formula $Ns = V/al_c$, where V is volume of hydrocarbon of head group, 'a' is the surface area of head group of surfactant, lc is the chain length of hydrocarbon. There is an effective variation in force generated during the surfactant aggregation and acting simultaneously on different molecules (water, surfactants, oils) and decides the structure of the micro-emulsion. Among different types of structure of micelles, in case of o@w µ-emulsion the spherical structure with hydrocarbon core can be obtained by the following equation: R =3V/a, where R is the spherical radius of the micelle. The radius of the spherical micelle cannot exceed a certain critical length l_c, so from this equation it can be deduced that when $V/al_c > 1/3$, the formation of spherical micelles are prohibited, giving a critical condition for the formation of sphere as $V/al_c = 1$.

2.3. Type of co-surfactant.

Co-surfactant presence signifies in the nanoparticle size determination of the nanoparticle. For the appropriate packing of surfactants, co-surfactants are added to it. Co-surfactants are generally short chain alcohols or amines. Co-surfactant lowers the interfacial tension between oil and water and reduces the surfactant concentration in µ-emulsion due to the "dilution effect". The particle size synthesized in µ-emulsion system is governed by the number of co-surfactants beside the bulkiness of oil that means the particle size increases with an increase in number of n-alcohol. Low molecular weight alcohols having short hydrophobic chain and terminal hydroxyl group increase the interaction with surfactant layer at the interface, hence, influence the curvature of the interface and internal energy. High radius of interfacial curvature radius of µ-emulsion droplet influences the intermicellar exchange. A high intermicellar exchange rate implies the more consumption of precursors at the nucleation stage thus, effective concentration reduces and thereby growth rate decreases and lastly particle size decreases. C. H. Lin et al. reported in his paper that with the increase in the volume n-hexanol the size of nanospheres (from 50 to 200nm) and shell thickness also increases [34]. Co-surfactant shows a pronounced effect on size distribution and stability of nanoparticle.

2.4. Water to surfactant ratio (Wo).

Water to surfactant ratio (Wo= $[H_2O]$/surfactant) determines size of the nanoparticle by increasing the micellarsize [35]. In water to surfactant ratio (Wo) is recognized when total water content is raised not only by increasing Wo but also increasing surfactant at constant Wo level [36]. Another consequence of altering Wo is to diverge the effective concentration of reagent inside the micelles, if the overall reagent concentration is kept constant throughout [37]. The variation in nanoparticle size is found due to the templating properties and physical constraints offered by micelles during nanoparticle growth [38].

3. DISCUSSIONS

Hao et al. synthesized (Zn–Ni) ferrite nanorods by an o@w µ-emulsion method at different calcine temperature (350, 500, 650, 800 and 900°C). Different molar ratio of Zn, Ni and Fe were prepared using a co-precipitation reaction of Zn^{2+}, Ni^{2+} and Fe^{3+} with $H_2C_2O_4$ in µ-emulsion solution [39]. The µ-emulsion was carried by taking surfactant/solvent/oil as (CTAB)/water/cyclohexane and here the co-surfactant given was n-pentanol. Then from the SEM it was confirmed that nanorods are formed of around 50–200 nm in diameter. It is clear that at different calcine temperature (350°C, 500°C, 650°C, 800°C, 900°C) the nanorod like morphology retained. The nanorod formation ($Zn_{0.5}$ $Ni_{0.5}Fe_2O_4$) is retained when the precursor is restricted within the $Zn_{0.5}Ni_{0.5}(C_2O_4)_3$. On calcinations, nucleation occurs and the growth process can be viewed when

$Zn_{0.5}Ni_{0.5}(C_2O_4)_3$ begins to decompose into $Zn_{0.5}Ni_{0.5}Fe_2O_4$. When the calcination temperature increases (350°C to 800°C), it lowers the number of particles and at the same time nanoparticle formation is much larger, indicating Ostwald ripening and oriented attachment process and the rods are 2 µm length. At higher calcine temperature (900°C), the $Zn_{0.5}Ni_{0.5}Fe_2O_4$ nanorod consists of individual crystal bound to each other. The diameter of the nanorod decreases with an increase in Zn content (0.1 to 0.9).

This is again confirmed from XRD that both the crystallinity and the average size of the crystallites increases with increasing calcinations temperature. The saturation magnetization MS gradually increases with increasing calcinations temperature. When Zn doping level increases from 0.1 to 0.5, the Ms (saturation magnetization) of samples increases. However with further increasing x value to 0.9, the Ms of $Zn_xNi_{1-x}Fe_2O_4$ nanorods decreases.

Three-dimensional (3D) hierarchical $PbWO_4$ microstructures were prepared by an o@w µ-emulsion-mediated route with three possible mechanistic step (nucleation, self-assembly and growth). For this study the emulsion was made by quaternary µ-emulsion system (sodium dodecyl benzene sulfonate (SDBS)/water/chloroform/1-pentanol) was selected. When the reaction is carried out at 100% water (without µ-emulsion) octahedral like structure with sunflower-like particle composed of a long nanobelt was formed. When the water content was reduced to 99 % and the rest 1% was chloroform is used in the reaction system, an octahedron with long strip like structure obtained. When SDBS is introduced into the reaction medium with 100% water, a non-uniform hierarchical microstructure formed. From this, it is clear that µ-emulsion has a unique contribution towards the determination of hierarchical microstructure. SEM image confirms a 3D hierarchical structure having six symmetric fishbone like arms (2-3µm each arm) and length about 1µm.To get a better 3D hierarchical $PbWO_4$ microstructure, time plays an important role. XRD results clear that at increased time (from 60 min to 4 hr), there is a gradual increase in intensity of diffraction peak. This suggests that crystallinity increases with increase in the reaction time. The formation and evolution of 3D hierarchical $PbWO_4$ involves three steps: a) nucleation process b) self assembly process and c) crystal growth process (Ostwald ripening). First, µ-emulsion plays a vital role and controls the rate of reaction and avoids the crystallographic fusion of the primary crystals to a single crystal. SDBS controls the growth of inhibition of different facts of $PbWO_4$ primary crystals. After certain strong interactions with the inorganic surface, a stabilized nanoparticle with surfactant coating form. This is regarded a "spherical core shell" nanoparticle with inorganic core and organic surfactant shell. In the self-assembly process, superstructures of $PbWO_4$ are formed through the interacting surfactants between the building blocks by sharing a common crystallographic interface which reduces the overall energy. Finally through the growth process (Ostwald ripening) 3D hierarchical $PbWO_4$ architectures with 6 symmetric fishbone arms irradiating from center [40].

Kao et al. synthesized of collapsed kippah like mesoporous silica nanoparticles using an o@w µ-emulsion system [41]. In this synthesis, MSN (Mesoporous silica nanoparticles) products were obtained by using an ammonia/cationic surfactant CTAB/TEOS/ethanol/water system in the following molar ratios: 0.36 CTAB / 1.0 TEOS / 244 ethanol / 3653 H_2O / 11 NH_3 / 2.1 alkane (decane, dodecane, and hexadecane). Different chain lengths of alkane, MSNs with different pore diameter were obtained was shown in TEM. In conventional MSN, without addition of alkane, spherical morphology obtained with diameter 100 nm. Again different morphologies are formed at different alkanes of the same molar concentration. The spherical shape changes to spindle-like structure, porous nanospheres structure and concave structure (kippah like) was formed by changing the alkane from decane, dodecane and hexadecane respectively. From the figure, it is clear that at a different alkyl chain length of alkane and altering the experimental procedures, a series of mesoporous silica materials with diverse morphologies can be obtained. In the schematic figure hexadecane is trapped by water droplets forming o@w micelles, after the addition of TEOS it forms silica shell to the droplet. The oil (hexadecane) can escape from the core while water could not enter through the surfactant filled nanopores of the soft shell. After that, the micro phase separation takes out the oil forming the kippah like mesoporous silica nanoparticles.

Preparation of polypyrrole (PPy) nanoparticles was achieved through o@w µ-emulsion method by Ovando-Medinan et al. [42]. The reaction was carried out by taking low surfactant concentration (SDS), ethanol as co-surfactant and low concentrations of the oxidizing agent potassium persulphate (KPS). Control of nanoparticle formation through µ-emulsion polymerization process is thermodynamically and kinetically unstable due to Ostwald ripening process. Herein, before polymerization, the µ–emulsion form with some of PPy dissolved in aqueous phase and appears as droplet, when SDS became higher than CMC. Alcohols (ethanol) act as an effective co-surfactant reduces the interfacial energy of monomer (pyrrole) droplet by interacting with polar heads of SDS and provides good solubility of pyrrole. When polymerization starts, radicals in aqueous phase are captured and some of the µ-emulsion droplet converted into particle.

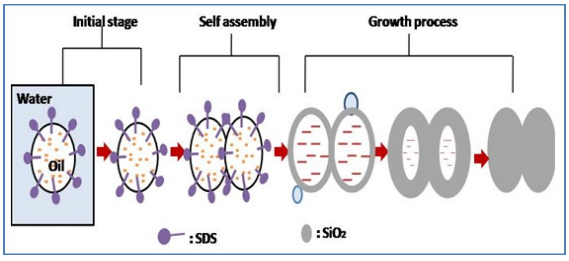

Figure-1. The representation of growth process of nanowire by o@w µ-emulsion.

Homogeneous nucleation provides the formation of a particle until a critical size reached. These precipitated radical can absorb the surfactant, self-stabilization enable to produce a stable polymer particle. The process will continue until µ–emulsion droplet disappears. The anionic surfactant (bi-polaron state) and the alcohol (longer effective π-conjugation) play an important role in morphology and electrical conductivity of PPy nanoparticles. By enhancing the ethanol concentration in the recipes, the conductive properties of the polymer increase confirmed from TEM image. The morphology illustrates that nanoparticles were

obtained through μ-emulsion polymerization arespherical in nature having average particle sizes were < 50 nm.

Jiang and his co-workers synthesized amorphous caddice-like silica nanowires (NWs) by self-assembly method through an o@w μ-emulsion scheme [43]. The morphology of silica nanostructures is controlled by taking the mass ratio of tetra ethyl ortho silicate to dimethyl benzene. Different reaction time (3min, 8min, 15 min, 60 min) plays a vital role in the formation of silica nanowires, confirmed through TEM. In the first stage (at 3 min), hollow sphere formed having diameter 67 nm with thin shell. As the time extends to 8 minute, there is a clear uneven rough surface of hypo genetic nanowires formed with slight increase in its diameter to 70nm. At 15 min. time, full growth of nanowire with uniform size was obtained. When there is a prolonged increased in time (60 min), a full grown nanowire with small burr was formed with mean diameter 82 nm. Three main possible mechanisms enhance the growth of nanowires. At first during the process of hydrolysis and condensation of TEOS occurred at the interface continuously. When more TEOS molecule migrated towards the oil/water interface, surface oil droplets formed solid porous shell of silica.

In the second stage, these porous shells were collide with each other and oil droplets were connected to each other and would not separate easily. These multiple oil droplets connected together and form a bigger droplet. The oil droplet with porous shell link together and gradual self-assembled to form a caddice like structure. In the third stage growth process many oil droplets of small size integrated and formed into a hollow porous nanowire. In the interior of the nanowire the liquid TEOS continuously react and solid silica was generated until the hollow porous nanowire was completely packed. The schematic diagram is shown in Figure 1. From this, it is clear that self-assembly and growth process are two key factors and occurs simultaneously for the formation of a complete solid nanowire. Lentz et al. observed one dimensional structure due to the short range interactions [44]. Other nanostructured materials are enlisted in Table 1 below.

Table 1. Different structure of nanocomposites synthesized through o@w μ-emulsion method.

S. No	Surfactant	Solvent	Oil	Cosurfactant	Precursors	Structure	References
1	CTAB	Water	Cyclohexane	n-pentanol	$ZnSO_4$,$NiSO_4$, $FeSO_4$	Rod	39
2	CTAB	Water	Decane, Hexadecane, Dodecane			Kippah hollow	41
3	NP-9	Water	Chloroform		TEOS, PTMS, APTES	Sphere	45
4	DBSA/AOT	Water	Cyclohexane	Hexanol, Butanol, Butanoic acid	Lipase, n-ethyl butyrate		46
5	SDBS	Water	chloroform	1-pentanol	$Pb(NO_3)_2$, $Na_2WO_4.2H_2O$	3D Symmetric fishbone	40
6	Brij-96	Water	Castor oil	Nil	Silver stearate, germanium leaf	Nanosphere	47
7	Sunlipon-90 Tween-80	Water	Sunflower oil	Nil	Phospholipids	Spherical nanodrop	48
8	Tween-80	Water	Fish oil, Hexadecane	Nil	Sodium azide, sodium phosphate buffer	Nanodrop	49
9	SDS	Water	Nil	Nil	Pyrrole,$(NH_4)_2S_2O_8$, Alcohol	Spherical particles	50
10	DTAB,MTAB, CTAB	Water	Nil	Nil	Pyrrole,$FeCl_3$,Iodine,MMA	Nanosphere	51
11	SDS	Water	DMB	n-Butanol		Nanowire	43
12	SDS	Water	KPS	Ethanol	Ppy	Sphere	42
13	Igepal co-520	Water	Cyclohexane	Nil	Ni $(NO_3)_2.6H_2O$, $(Mg(NO_3)_2.6H_2O)$	Nnaorod	52
14		Water	Oleic acid	Nil	$AgNO_3$, TBM, OVA, ammonium acetate	Hollow	53
15	CTAB	Water	Ethylacetate	Ethanol	TEOS, APTES, $HAuCl_4$	Trilobite	54

4. CONCLUSIONS

The parameters used in o@w micro-emulsion (type of oil, surfactants, co-surfactants, water to surfactant ratio, temperature, time, and type of precursors) along with optimization of reaction condition make the process unique in the formation of nanostructured materials. Apart from these three unique step involved in the growth mechanism of nanostructure material includes the o@w emulsion (nucleation, self-assembly, i.e orientated aggregation and subsequent crystal growth) enable the material to produce indifferent shape and sizes. In this regard, the synthesis of different shape and size of nanostructured material through o@w micro-emulsion is no doubt is better than utilization of high-end fine chemicals. This approach may increase the potential of the synthesis of micro/nanostructures through micro-emulsion reaction technique, and its scale can be extended to cover the preparation of other inorganic materials with a complex morphology. Applications of this approach in the fields materials science are expected.

5. REFERENCES

1. Malik, M.A.; Wani, M.Y.; Hashim, M.A. Microemulsion method: A novel route to synthesize organic and inorganic nanomaterials: 1st Nano Update. *Arabian journal of Chemistry* **2012**, *5*, 397-417, https://doi.org/10.1016/j.arabjc.2010.09.027.
2. Schwarze, M.; Pogrzeba, T.; Volovych, I.; Schomäcker, R. Microemulsion systems for catalytic reactions and processes. *Catalysis Science & Technology* **2015**, *5*, 24-33, https://doi.org/10.1039/C4CY01121J.
3. Wang, J.; Shah, Z.H.; Zhang, S.; Lu, R. Silica-based nanocomposites via reverse microemulsions: classifications, preparations, and applications. *Nanoscale* **2014**, *6*, 4418-4437, https://doi.org/10.1039/C3NR06025J.
4. Jeevanandam, J.; Barhoum, A.; Chan, Y.S.; Dufresne, A., Danquah, M.K. Review on nanoparticles and nanostructured materials: history, sources, toxicity and regulations. *Beilstein J. Nanotechnol.* **2018**, *9,* 1050–1074, https://doi.org/doi:10.3762/bjnano.9.98.
5. Lombardo, D.; Kiselev, A.M.; Caccamo, M.T. Smart Nanoparticles for Drug Delivery Application: Development of Versatile Nanocarrier Platforms in Biotechnology and Nanomedicine**.** *Hindawi Journal of Nanomaterials* **2019**, *2019*, https://doi.org/10.1155/2019/3702518.
6. Patra, J.K.; Das, G.; Fraceto, L.F.; Campos, E.V. Ramos., Rodriguez-Torres M. del P., Acosta-Torres, L. S., Diaz-Torres, L. A., Grillo R., Kumara Swamy, M., Sharma, S., Habtemariam, S., and Shin, H. S., Nano based drug delivery systems: recent developments and future prospects. *J Nanobiotechnol.* **2018**, *16*, https://doi.org/10.1186/s12951-018-0392-8.
7. Azcona, P.; Zysler, R.; Lassalle, V. Simple and novel strategies to achieve shape and size control of magnetite nanoparticles intended for biomedical applications. *Colloids and Surfaces A: Physicochemical and Engineering Aspects* **2016**, *504*, 320-330, https://doi.org/10.1016/j.colsurfa.2016.05.064.
8. Richard, B.; Lemyre, J.L.; Ritcey, A.M. Nanoparticle size control in microemulsion synthesis. *Langmuir* **2017**, *33*, 4748-4757, https://doi.org/10.1021/acs.langmuir.7b00773.
9. Chen, P.C.; Mwakwari, S.C.; Oyelere, A.K. Gold nanoparticles: from nanomedicine to nanosensing. *Nanotechnology, science and applications* **2008**, *1***,** 45-65, https://doi.org/10.2147/nsa.s3707.
10. Fuke, M.V.; Kanitkar, P.; Kulkarni, M.; Kale, B.B.; Aiyer, R.C. Effect of particle size variation of Ag nanoparticles in Polyaniline composite on humidity sensing. *Talanta* **2010**, *81*, 320-326, https://doi.org/10.1016/j.talanta.2009.12.003.
11. Gross, J.; Sayle, S.; Karow, A.R.; Bakowsky, U.; Garidel, P. Nanoparticle tracking analysis of particle size and concentration detection in suspensions of polymer and protein samples: influence of experimental and data evaluation parameters. *European Journal of Pharmaceutics and Biopharmaceutics* **2016**, *104*, 30-41, https://doi.org/10.1016/j.ejpb.2016.04.013.
12. Sahoo, D.P.; Rath, D.; Nanda, B.; Parida, K.M. Transition metal/metal oxide modified MCM-41 for pollutant degradation and hydrogen energy production: a review. *RSC Advances* **2015**, *5*, 83707-83724, https://doi.org/10.1039/C5RA14555D.
13. Melo, R.S.; Banerjee, P.; Franco, A. Hydrothermal synthesis of nickel doped cobalt ferrite nanoparticles: optical and magnetic properties. *Journal of Materials Science: Materials in Electronics* **2018**, *29*, 14657-14667, https://doi.org/10.1007/s10854-018-9602-2.
14. Rajput, N. Methods of preparation of nanoparticles-A review. *International Journal of Advances in Engineering & Technology* **2015**, *7*, 1806-1811.
15. Wang, H.; Qiao, X.; Chen, J.; Ding, S. Preparation of silver nanoparticles by chemical reduction method. *Colloids and Surfaces A: Physicochemical and Engineering Aspects* **2005**, *256*, 111-115, https://doi.org/10.1016/j.colsurfa.2004.12.058.
16. Xu, H.; Zeiger, B.W.; Suslick, K.S. Sonochemical synthesis of nanomaterials. *Chemical Society Reviews* **2013**, *42*, 2555-2567, https://doi.org/10.1039/C2CS35282F.
17. Rojas, S.; Eriksson, S.; Boutonnet, M.; Spivey, J.J.; Roberts, G.W. Microemulsion: An alternative route to preparing supported catalysts. *Catalysis* **2004**, *17*, 258-292.
18. Malik, M.A.; Wani, M.Y.; Hashim, M.A. Microemulsion method: A novel route to synthesize organic and inorganic nanomaterials: 1st Nano Update. *Arabian journal of Chemistry*, **2012**, *5*, 397-417, https://doi.org/10.1016/j.arabjc.2010.09.027.
19. McClements, D.J. Nanoemulsions versus microemulsions: terminology, differences, and similarities. *Soft matter* **2012**, *8*, 1719-1729, https://doi.org/10.1039/C2SM06903B.
20. Wolf, L.; Hoffmann, H.; Linders, J.; Mayer, C. PFG-NMR self-diffusion measurements in the single phase channels of a microemulsion system with an anionic–nonionic surfactant mixture. *Soft Matter* **2012**, *8*, 6731-6739, https://doi.org/10.1039/C2SM07301C.
21. Zang, J.; Feng, M.; Zhao, J.; Wang, J. Micellar and bicontinuous microemulsion structures show different solute–solvent interactions: a case study using ultrafast nonlinear infrared spectroscopy. *Physical Chemistry Chemical Physics* **2018**, *20*, 19938-19949, https://doi.org/10.1039/C8CP01024B.
22. Lamiel-Garcia, O.; Cuko, A.; Calatayud, M.; Illas, F.; Bromley, S. T. Predicting size-dependent emergence of crystallinity in nanomaterials: titania nanoclusters versus nanocrystals. *Nanoscale* **2017**, *9*, 1049-1058, https://doi.org/10.1039/C6NR05788H.
23. Zhu, Q.; Qiu, S.; Zhang, H.; Cheng, Y.; Yin, L. Physical stability, microstructure and micro-rheological properties of water-in-oil-in-water (W/O/W) emulsions stabilized by porcinegelatin. *Foodchemistry* **2018**, *253*, 63-70, https://doi.org/10.1016/j.foodchem.2018.01.119.
24. Ganguli, A.K.; Ganguly, A.; Vaidya, S. Microemulsion-based synthesis of nanocrystalline materials. *Chemical Society Reviews*, *39*, 474-485, https://doi.org/10.1039/B814613F.
25. Tang, A.Y.; Lee, C.H.; Wang, Y.M.; Kan, C.W. Effect of hydrophilic-lipophilic balance (HLB) values of PEG-based non-ionic surfactant on reverse micellar dyeing of cotton fibre with reactive dyes in non-aqueous medium. *Fibers and Polymers* **2018**, *19*, 894-904, https://doi.org/10.1007/s12221-018-8061-y.
26. Paul, B.K.; Moulik, S.P. Uses and applications of microemulsions. *Current science* **2001**, *80*, 990-1001.
27. Hao, L.; Zhao, Y.; Jiao, Q.; Chen, P. Synthesis of zinc–nickel ferrite nanorods and their magnetic properties. *RSC Advances* **2014**, *4*, 15650-15654, https://doi.org/10.1039/C3RA47780K.
28. Amirthavalli, C.; Thomas, J.M.; Nagaraj, K.; Prince, A.A.M. Facile room temperature CTAB-assisted synthesis of mesoporous nano-cobalt ferrites for enhanced magnetic behaviour. *Materials Research Bulletin* **2018**, *100*, 289-294, https://doi.org/10.1016/j.materresbull.2017.12.026.
29. Mcclements, D.J. Critical review of techniques and methodologies for characterization of emulsion stability. *Critical reviews in food science and nutrition* **2007**, *47*, 611-649, https://doi.org/10.1080/10408390701289292.
30. Palazzo, G.; Lopez, F.; Giustini, M.; Colafemmina, G.; Ceglie, A. Role of the cosurfactant in the CTAB/water/n-pentanol/n-hexane water-in-oil microemulsion. 1. Pentanol effect on the microstructure. *The Journal of Physical Chemistry B* **2003**, *107*, 1924-1931, https://doi.org/10.1021/jp026430o.
31. Chaiyana, W.; Rades, T.; Okonogi, S. Characterization and in vitro permeation study of microemulsions and liquid crystalline systems containing the anticholinesterase alkaloidal extract from Tabernaemontana divaricata. *International journal of pharmaceutics* **2013**, *452*, 201-210, https://doi.org/10.1016/j.ijpharm.2013.05.005.

32. LaMer, V.K.; Dinegar, R.H. Theory, production and mechanism of formation of monodispersed hydrosols. *Journal of the American Chemical Society* **1950**, *72*, 4847-4854, https://doi.org/10.1021/ja01167a001.
33. Tauer, K.; Ramírez, A.G.; López, R.G. Effect of the surfactant concentration on the kinetics of oil in water microemulsion polymerization: a case study with butyl acrylate. *Comptes Rendus Chimie* **2003**, *6*, 1245-1266, https://doi.org/10.1016/j.crci.2003.06.008.
34. Lin, C.H.; Chang, J.H.; Yeh, Y.Q.; Wu, S.H.; Liu, Y.H.; Mou, C.Y. Formation of hollow silica nanospheres by reverse microemulsion. *Nanoscale* **2015**, *7*, 9614-9626, https://doi.org/10.1039/C5NR01395J.
35. Granata, G.; Pagnanelli, F.; Nishio-Hamane, D.; Sasaki, T. Effect of surfactant/water ratio and reagents' concentration on size distribution of manganese carbonate nanoparticles synthesized by microemulsion mediated route. *Applied Surface Science* **2015**, *331*, 463-471, https://doi.org/10.1016/j.apsusc.2015.01.101.
36. Pileni, M.P. Control of the size and shape of inorganic nanocrystals at various scales from nano to macrodomains. *The Journal of Physical Chemistry C* **2007,** *111*, 9019-9038, https://doi.org/10.1021/jp070646e.
37. Richard, B.; Lemyre, J.L.; Ritcey, A.M. Nanoparticle size control in microemulsion synthesis. *Langmuir* **2017,** *33*, 4748-4757, https://doi.org/10.1021/acs.langmuir.7b00773.
38. Sajanlal, P.R.; Sreeprasad, T.S.; Samal, A.K.; Pradeep, T. Anisotropic nanomaterials: structure, growth, assembly, and functions. *Nano reviews* **2011**, *2*, 1-62, https://doi.org/10.3402/nano.v2i0.5883.
39. Hao, L.; Zhao, Y.; Jiao Q.; Chen, P. Synthesis of zinc–nickel ferrite nanorods and their magnetic properties. *RSC Advances* **2014**, *4*, 15650-15654, https://doi.org/10.1039/c3ra47780k.
40. Tang, H.; Li, C.; Song, H.; Yang, X.; Yan, X. Controllable synthesis, characterization and growth mechanism of three-dimensional hierarchical $PbWO_4$ microstructures. *CrystEngComm* **2011**, *13*, 5119-5124, https://doi.org/10.1039/C1CE05060E.
41. Kao, K.C.; Tsou C.J.; Mou, C.Y. Collapsed (kippah) hollow silica nanoparticles. *Chemical Communications* **2012**, *48*, 3454-3456, https://doi.org/10.1039/c2cc30411b.
42. Ovando-Medina, V.M.; Peralta, R.D.; Mendizábal, E.; Martínez-Gutiérrez, H.; Lara-Ceniceros, T.E.; Ledezma-Rodríguez, R. Synthesis of polypyrrole nanoparticles by oil-in-water microemulsion polymerization with narrow size distribution. *Colloid and Polymer Science* **2011**, *289*, 759-765, https://doi.org/10.1007/s00396-011-2394-z.
43. Jiang, D.; Deng, Y.; Gao, G.; Wu, L.; Yang, H. Self-assembly of silica nanowires in a microemulsion system and their adsorption capacity. *Colloids and Surfaces A: Physicochemical and Engineering Aspects* **2018**, *538*, 526-533, https://doi.org/10.1016/j.colsurfa.2017.11.014.
44. Lenz, M.; Witten, T.A. Geometrical frustration yields fibre formation in self-assembly. *Nature physics* **2017**, *13*, 1100-1104, https://doi.org/10.1038/nphys4184.
45. Kong, L.; Uedono, A.; Smith, S.V.; Yamashita, Y.; Chironi, I. Synthesis of silica nanoparticles using oil-in-water emulsion and the porosity analysis. *Journal of sol-gel science and technology* **2012**, *64*, 309-314, https://doi.org/10.1007/s10971-012-2859-7.
46. Han, Y.; Chu, Y. The catalytic properties and mechanism of cyclohexane/DBSA/water microemulsion system for esterification. *Journal of Molecular Catalysis A: Chemical* **2005**, *237*, 232-237, https://doi.org/10.1016/j.molcata.2005.04.058.
47. Rivera-Rangel, R.D.; González-Muñoz, M.P.; Avila-Rodriguez, M.; Razo-Lazcano T.A.; Solans, C. Green synthesis of silver nanoparticles in oil-in-water microemulsion and nano-emulsion using geranium leaf aqueous extract as a reducing agent. *Colloids and Surfaces A: Physicochemical and Engineering Aspects*, **2018**, *536*, 60-67, http://dx.doi.org/doi:10.1016/j.colsurfa.2017.07.051.
48. Komaiko, J.; Sastrosubroto, A.; McClements, D.J. Formation of oil-in-water emulsions from natural emulsifiers using spontaneous emulsification: sunflower phospholipids. *Journal of agricultural and food chemistry*, **2015**, *63*, 10078-10088, https://doi.org/10.1021/acs.jafc.5b03824.
49. Erdmann, M.E.; Zeeb, B.; Salminen, H.; Gibis, M.; Lautenschlaeger, R.; Weiss, J. Influence of droplet size on the antioxidant activity of rosemary extract loaded oil-in-water emulsions in mixed systems. *Food & function* **2015,** *6*, 793-804, https://doi.org/10.1039/C4FO00878B.
50. Liu, Y.; Chu, Y.; Yang, L. Adjusting the inner-structure of polypyrrole nanoparticles through microemulsion polymerization. *Materials chemistry and physics* **2006**, *98*, 304-308, https://doi.org/10.1016/j.matchemphys.2005.09.025.
51. Jang J.; Oh, J.H. Fabrication of a highly transparent conductive thin film from polypyrrole/ploy (methyl methacrylate) core/shell nanospheres. *Advance Functional Matererial* **2005,** *15*, 494-502, https://doi.org/10.1002/adfm.200400095.
52. Usman, M.; Daud, W.W. Microemulsion based synthesis of Ni/MgO catalyst for dry reforming of methane. *RSC Advances* **2016**, *6*, 38277-38289, https://doi.org/10.1039/c6ra01652a.
53. Ethayaraja, M.; Dutta, K.; Muthukumaran, D.; Bandyopadhyaya, R. Nanoparticle formation in water-in-oil microemulsions: experiments, mechanism, and Monte Carlo simulation. *Langmuir* **2007**, *23*, 3418-3423, https://doi.org/10.1021/la062896c.
54. Pak, J.; Yoo, H. Facile synthesis of spherical nanoparticles with a silica shell and multiple Au nanodots as the core. *Journal of Materials Chemistry A* **2013**, *1*, 5408-5413, https://doi.org/10.1039/C3TA10613F.

6. ACKNOWLEDGEMENTS

Authors are thankful to the management SOA (deemed to be University) for constant encouragement.